Plant and Soil (2005) 276:115–132
DOI 10.1007/s11104-005-3504-9
© Springer 2005

Goethite dissolution in the presence of phytosiderophores: rates, mechanisms, and the synergistic effect of oxalate

P.U. Reichard[1], S.M. Kraemer[1,2], S.W. Frazier[1] & R. Kretzschmar[1]
[1]*Department of Environmental Sciences, ETH Zürich, Grabenstrasse 3, 8952 Schlieren, Switzerland.* [2]*Corresponding author**

Received 30 November 2004. Accepted in revised form 10 March 2005

Key words: deoxymugineic acid, dissolution mechanism, iron oxide, strategy II, *Triticum aestivum*, weathering kinetics

Abstract

The purpose of this study was the elucidation of the chemical mechanism of an important process in iron acquisition by graminaceous plants: the dissolution of iron oxides in the presence of phytosiderophores. We were particularly interested in the effects of diurnal root exudation of phytosiderophores and of the presence of other organic ligands in the rhizosphere of graminaceous plants on the dissolution mechanism. Phytosiderophores of the type 2′-deoxymugineic acid (DMA) were purified from the root exudates of wheat plants (*Triticum aestivum* L. cv. Tamaro). DMA-promoted dissolution of goethite under steady-state and non-steady-state conditions and its dependence on pH, adsorbed DMA concentration, and the presence of the organic ligand oxalate were studied. We show that dissolution of goethite by phytosiderophores follows a surface controlled ligand promoted dissolution mechanism. We also found that oxalate, an organic ligand commonly found in rhizosphere soils, has a synergistic effect on the steady-state dissolution of goethite by DMA. Under non-steady-state addition of the phytosiderophore, mimicking the diurnal exudation pattern of phytosiderophore release, a fast dissolution of iron is triggered in the presence of oxalate. To investigate the efficiency of these mechanisms in plant iron acquisition, wheat plants were grown on a substrate amended with goethite as only iron source. The chlorophyll status of these plants was similar to iron-fertilized plants and significantly higher than in plants grown in iron free nutrient solutions. This demonstrates that wheat can efficiently mobilize iron, even from well crystalline goethite that is usually considered unavailable for plant nutrition.

Introduction

Iron deficiency in crop plants is a widespread problem that occurs in many parts of the world. It is typically observed in well-drained calcareous soils in which iron solubility is extremely low due to high soil pH. In the neutral to alkaline pH range that is characteristic for such soils, the concentration of inorganic iron species in equilibrium with soil iron oxides is less than 2 nM (Lindsay, 1979). This equilibrium iron concentration is orders of magnitude lower than the plant requirement for adequate iron nutrition as estimated from hydroponic culture experiments (Marschner, 1995). Considering this, the occurrence of plant iron deficiency seems to be inevitable, unless specific iron uptake strategies are available to iron stressed plants. For example, it was found that crop relevant species among the group of graminaceous plants (e.g., barley and wheat) were less susceptible to iron deficiency in calcareous soils than other, non-graminaceous species (Römheld and Marschner, 1986). Detailed investigations on iron acquisition by graminaceous plants demonstrated that their iron mobilizing strategy is completely different from that of

* FAX No: +41-44-633-1118. E-mail: kraemer@env.ethz.ch

all other monocotyledons and the dicotyledons (Takagi et al., 1984). This so-called strategy II (Marschner et al., 1986) involves the production and exudation of phytosiderophores induced by iron deficiency and the mobilization of Fe^{3+} from sparingly soluble inorganic Fe(III) phases. Dissolved Fe(III) is taken up as iron-phytosiderophore complex via specific transporter systems in the roots (Römheld, 1991).

Besides the exudation of phytosiderophores, graminaceous plants secrete other organic ligands into the rhizosphere. The exudation of such organic ligands has been suggested as part of strategy I plant iron acquisition (Jones et al., 1996; Marschner, 1995). Dakora and Phillips (2002) reported the exudation of malate by wheat and Vančura (1964) reported the exudation of oxalate by wheat. Fan et al. (1997) observed the root exudation of iron stressed barley plants and found that not only phytosiderophore secretion was increased but also the exudation of diverse amino acids and carboxylates, including fumarate and malate. Based on these observations they speculated that low molecular weight organic ligands could also be involved in nutrient mobilization by plants.

In the last few years, several studies were carried out on the formation of phytosiderophores (Higuchi et al., 1999; Nakanishi et al., 1999; Higuchi et al., 2001;), on their exudation (Singh et al., 2000; Negishi et al., 2002; Ma et al., 2003), and on the uptake mechanism of iron-siderophore complexes. Other studies focused on the effects of phytosiderophores on iron oxide solubility and dissolution. Takagi et al. (1988) observed that phytosiderophores were more effective in extracting iron from calcareous soils than the microbial siderophore desferrioxamine B (DFO-B) or synthetic chelates (e.g., EDTA). In dissolution experiments with synthesized iron (hydr)oxides, Inoue et al. (1993) found that phytosiderophores dissolved ferrihydrite with maximum dissolution rates at pH 7 and 8, but much less goethite dissolution was observed. Hiradate and Inoue (1998) also observed significant dissolution of iron by phytosiderophores at higher pH values mainly for ferrihydrite. It was suggested by Awad et al. (1994) that a high crystallinity of iron(oxyhydr)oxides inhibits iron mobilization by phytosiderophores. On the other hand, Bertrand and Hinsinger (2000) found a re-greening of chlorotic maize that was fed with goethite as the only iron source. Since maize did not increase the pool of DTPA-extractable iron, but only depleted the oxalate extractable iron pool, they suggested that maize could only mobilize iron from amorphous iron phases being present in the goethite as contaminations.

In this study, we investigated the interactions between phytosiderophores and the iron oxyhydroxide goethite (α-FeOOH) that represents one of the most abundant iron phases in soils (Matar et al., 1992; Cornell and Schwertmann, 2003). This investigation was designed to shed light on the thermodynamics and the kinetics of important geochemical processes in the context of plant iron acquisition in a pH range relevant for the development of iron deficiency.

Phytosiderophore exudation by plant roots can vary in time and space. The release of siderophores varies along the root and is most pronounced in apical root zones (Marschner et al., 1987). Also, it is often observed that phytosiderophore exudation by graminaceous plants follows a diurnal exudation pattern (Takagi et al., 1984; Marschner et al., 1986) starting about 2 h after sunrise and lasting for a few hours. Such distinct diurnal patterns for the excretion of root exudates (Stewart and Lieffers, 1994; Hagström et al., 2001;), but also for the translocation of iron (Alam et al., 2004) were described for various plant species. Exceptional continuous exudation of phytosiderophores by *Zea mays* L. cv. Alice has been observed (Yehuda et al., 1996). Interestingly, there is no indication that diurnal phytosiderophore exudation decreases the efficiency of the Fe acquisition mechanisms relative to continuous exudation, despite the short time available for iron mobilization and uptake. To investigate the effect of this pulse-like, diurnal phytosiderophore exudation on the dissolution of goethite, we carried out experiments under non-steady-state conditions. We used oxalate as a model compound to elucidate the effect of low molecular weight organic ligands on these processes. Most studies on graminaceous root exudation do not report oxalate in root washings. However, oxlate is found in a wide range of soil types including cultivated soils (Graustein and

Cromack, 1977; Jones. 1998; Gadd, 2000; Strobel, 2001). Most root exudates, including monodentate carboxylate ligands, have a low affinity for iron complexation. However, di- and tri-carboxylates and hydroxycarboxylates such as citrate, oxalate, malate, fumarate and tartarate have a significant affinity for iron complexation in solution and at iron oxide surfaces (Filius et al., 1997; Jones and Brassington, 1998).

Wheat was chosen as model plant for these investigations due to its importance as crop plant and for its high tolerance to iron deficiency due to high phytosiderophore production rates (Ma and Nomoto, 1996). Furthermore, wheat produces primarily one single phytosiderophore of the mugineic acid family, namely DMA (2′-deoxymugineic acid) (Sugiura and Nomoto, 1984; Takagi, 1993; Mori, 1994; Ma et al., 1995).

A series of dissolution experiments was designed to elucidate the mechanisms and rates of phytosiderophore promoted dissolution of goethite. We investigated the effect of oxalate on this process under steady-state and non-steady-state conditions. Also, plant growth experiments were conducted to test the ability of wheat to acquire iron from the crystalline oxyhydroxide goethite.

Materials and methods

Materials

Goethite was synthesized following the method of Schwertmann and Cornell (2000). X-ray powder diffraction confirmed the goethite structure and no impurities were observed. The specific surface area of the goethite was 38 $m^2\,g^{-1}$, determined by a multipoint N_2–BET method (Gemini 2360, Micromeritics, Norcross, USA).

All dissolution and adsorption experiments were performed in 0.01 *M* $NaClO_4$ (sodium perchlorate monohydrate; Merck, Darmstadt, Germany) or 0.01 *M* $NaNO_3$ (sodium nitrate; Merck, Darmstadt, Germany) buffered in the pH range between 5 and 9 with 0.005 *M* MOPS (3-morpholinepropanesulfonic acid; Fluka, Buchs, Switzerland) unless otherwise noted. MOPS was found to have no influence on the dissolution of goethite by the microbial siderophore desferrioxamine B (Kraemer et al., 1999) and Yu et al. (1997) showed that MOPS does not complex trace metal ions. Oxalate (di-sodium oxalate; Merck, Darmstadt, Germany) was used as received. The pH of the solutions and suspensions were adjusted with perchloric acid and sodium hydroxide, respectively. All solutions were prepared with high-purity deionized water (18 MΩ, Milli-Q, Millipore, Billerica, USA).

For Fe-DMA adsorption experiments, a Fe-stock solution of 0.5 m*M* dissolved Fe^{3+} acidified with perchloric acid was prepared from $FeCl_3$ (iron(III)chloride hexahydrate; Merck, Darmstadt, Germany).

Fe-EDTA (ethylenediaminetetraacetic acid, iron(III) sodium salt hydrate; Fluka, Buchs, Switzerland) and DMF (N,N-dimethylforamide; Merck, Darmstadt, Germany) used in the pot experiments were analytical grade and used as received.

Collection and purification of phytosiderophores

Phytosiderophores were isolated from root exudates of iron deficient wheat plants (*Triticum aestivum* L. cv. Tamaro) grown in hydroponic culture in a climate controlled chamber. The nutrient solution was prepared following the recipe of Neumann et al. (1999) and contained no iron. The day/night regime of the growth chamber was 16/8 h at 21/18°C, with a photon flux of 327 $\mu mol\,m^{-2}\,s^{-1}$ and a relative humidity of 65%. After about 14 days, the plants showed visible signs of chlorosis and the collection of root exudates was started. The exudate collection and phytosiderophore purification were performed after the method of Neumann et al. (1999). Briefly, root exudates were collected by immersing the pre-washed roots in suprapure water during the daily exudation period. Microbial growth was suppressed by adding Micropure® tablets (Katadyn, Wallisellen, Switzerland) to the solutions immediately after collection. After filtration (60 and 30 μm filters (Balston, Haverhill, USA)) the solutions were loaded on a preparative cation exchange column (Dowex 50 WX2, Serva, Heidelberg, Germany) and eluted with 2 *M* HCl. To remove the acid and to reduce the volume of the eluted phytosiderophore fraction, the solution

was evaporated at 50°C in a rotary evaporator (Büchi, Flawil, Switzerland). Further purification and desalting was performed by size exclusion chromatography (Sephadex G−10, Amersham Pharmacia, Freiburg, Germany) using a preparative column (1.7 cm ID × 50 cm). Finally, metal ions were removed using a column (3.2 cm ID × 19 cm) of chelating resin (Chelex 100, Bio-Rad, Reinach, Switzerland). After the purification, the phytosiderophores were freeze dried. The product was >98% 2′-deoxymugineic acid as verified with ^{1}H-NMR and ^{13}C-NMR (400 MHz, D_2O, RT) (Reichard, 2005). Stock solutions were prepared using the purified DMA for further use in dissolution and adsorption experiments.

Plant growth experiments

The ability of wheat (*Triticum aestivum* L. cv. Tamaro) to acquire iron from goethite was tested in pot experiments. Six wheat plants were germinated in saturated $CaSO_4$ solution in the dark. After development of the first leaf (Feekes growth stage 1.1; Large, 1954), two plants were transferred in each of three HDPE (high density polyethylene) pots filled with 140 g of PTFE (teflon) plastic beads (Glorex, Rheinfelden, Germany) with different diameters ranging from 1–2 mm. Before using the plastic beads, they were washed with 1 *M* HCl for one day and then rinsed with DI water until neutral pH was reached. In pot experiments, plants were exposed to three different treatments. In treatment 1 and 3, the plants were fed with an iron-free nutrient solution at pH 6. In treatment 2, plants were fed with the same nutrient solution to which 0.1 m*M* Fe-EDTA was added as iron source. In treatment 3, the plastic beads were mixed homogeneously with 1 g goethite as iron source. Before planting the wheat seedlings into the pots, the plastic beads were equilibrated with the nutrient solutions.

The pot experiments were performed in a climate controlled chamber (conditions see above) for 15 days. Nutrient solutions were added by drip irrigation during the dark period with a flow rate of 4 mL h^{-1}. The flow rates were controlled by a peristaltic pump. The upper parts of the pots that were not in contact with the nutrient solution were wrapped in aluminum foil to suppress algal growth and to prevent photochemical dissolution of goethite in treatment 3. After development of the second leaf (Feekes growth stage 1.2, Large, 1954), chlorophyll measurements were performed once a day to monitor the iron nutrition of the plants. The chlorophyll measurements were conducted with a leaf chlorophyll-meter (SPAD 502; Minolta, Tokyo, Japan). The chlorophyll-meter was calibrated using the chlorophyll determination method of Moran (1982). After 15 days, the plants were harvested and the biomass of the shoots was determined.

Dissolution experiments

Two types of dissolution experiments were conducted: steady-state and non-steady-state batch dissolution experiments. For the steady-state dissolution experiments, goethite suspensions with a goethite concentration of 2.5 g L^{-1}, an ionic strength of 0.01 *M* buffered to a pH of 5.0, 6.0, 7.0, 8.0 or 9.0 ± 0.05 were prepared. Dissolution experiments at pH 6 contained either 0 or 100 μM oxalate. At time $t = 0$, DMA concentrations of 10, 50, 150, 350, 500 or 3000 μM were added to the suspensions. Non-steady-state batch dissolution experiments were conducted analogous to steady-state experiments except for delayed additions ($t > 0$) of small volumes of a concentrated DMA stock solution to reach final concentrations of 3 m*M*. Non-steady-state dissolution experiments were exclusively performed at pH 6.

The batch reactors consisted of 20 mL polypropylene containers, wrapped with aluminum foil to exclude light. The reactors were shaken continuously on an end-over-end shaker at ambient temperature. Samples were taken intermittently over time and filtered using plastic syringe filter holders (Schleicher & Schuell, Dassel, Germany; Millipore, Billerica, USA) with 0.025 μm cellulose nitrate membranes (Schleicher & Schuell, Dassel, Germany). The first 10 μL of the filtrate were discarded and 1 mL was collected and immediately frozen.

To investigate competitive adsorption of oxalate and DMA at the goethite surface, a stock solution containing ^{14}C-labeled oxalate (250 μCi; Fluka, Buchs, Switzerland) together with

non-radioactive oxalate were added to a goethite-electrolyte suspension at pH 6 (solids concentration 2.5 g L^{-1}, ionic strength 0.01 *M* ($NaClO_4$), buffered with 0.005 *M* MOPS) to reach a final oxalate concentration of 100 μM. The concentration of ^{14}C-labeled oxalate was determined with a scintillation counter (Liquid Scintillation Analyzer 2200CA; Packard, Downers Grove, USA) and the total adsorbed oxalate concentration was calculated. Then, either 0.5 or 3 m*M* DMA were added and the concentration of ^{14}C-labeled oxalate was determined again. From the difference between the adsorbed oxalate concentration before and after the DMA addition, the displacement of oxalate by DMA at the goethite surface was calculated.

Adsorption isotherms

Adsorption isotherms for DMA on goethite were measured at pH 6 and 8. For each isotherm, two replicates of goethite-DMA suspensions and one series of blanks were prepared. The samples had goethite concentrations of 2.5 g L^{-1} for pH 6, and 15 g L^{-1} for pH 8. A higher solids concentration was used at pH 8 in order to measure low adsorbed surface concentrations expected at that pH with reasonable precision. The ionic strength was adjusted to 0.01 *M* using perchlorate for the pH 6 isotherm and using $NaNO_3$ for the pH 8 isotherm. The batch volume was 7 mL. Blanks were prepared analogously but without goethite. The total DMA concentrations were 5, 20, 50, 75, 100 and 300 μM at pH 6 and 25, 50, 150, 300, 500 and 700 μM at pH 8. After a reaction time of 0.5 h, the samples were filtered using plastic syringe filter holders (Schleicher & Schuell, Dassel, Germany) with 0.025 μm cellulose nitrate membranes (Schleicher & Schuell, Dassel, Germany). The first 2 mL of the filtrate were discarded, 1.5 mL were collected for phytosiderophore analysis with HPLC and 3.5 mL were collected for the determination of total dissolved iron with ICP-MS.

Adsorption isotherms for Fe-DMA adsorption on goethite were recorded at pH 5, 6, 7, 8 and 9. The samples had a goethite concentration of 2.5 g L^{-1}, an ionic strength of 0.01 *M* and were pH buffered with 0.005 *M* MOPS. The batch volume was 7 mL. The total DMA concentration was 500 μM. Total dissolved iron concentrations were 0, 3.5, 7, 10.5, 14, 21 and 28 μM for pH 6, and 0, 2.5, 5, 7.5, 10, 15 and 20 μM for pH 5, 7, 8, and 9. Equilibrium calculations (PHREEQC, Parkhurst and Appelo (1999)) were performed to ascertain that the solution was not over-saturated with respect to iron oxide phases to avoid surface precipitation (see Table 2 for equilibrium constants). Based on results of dissolution experiments, a reaction time of 0.5 h was chosen to minimize interferences by Fe dissolution in the course of the adsorption measurements. The samples were filtered using plastic syringe filter holders (Schleicher & Schuell, Dassel, Germany) with 0.025 μm cellulose nitrate membranes (Schleicher & Schuell, Dassel, Germany). The first 2 mL of the filtrate were discarded and 5 mL were collected for the determination of total dissolved iron with ICP-MS.

Adsorption envelope

To study the pH dependence of phytosiderophore adsorption on goethite, one series of blanks and two replicates of goethite suspensions were prepared at pH 5, 6, 7, 8, and 9. The batch volume was 5 mL. The ionic strength was adjusted to 0.01 *M* using $NaNO_3$. No pH buffer was added. The suspensions and blanks were spiked with 500 μM DMA and reacted for 1 h with constant pH-monitoring. Subsequently, the samples were filtered using plastic syringe filter holders (Schleicher & Schuell, Dassel, Germany) with 0.025 μm cellulose nitrate membranes (Schleicher & Schuell, Dassel, Germany).

Table 1. Freundlich parameters for the Freundlich isotherm model $Fe_{\mathrm{ads}} = K_d \cdot C^{\frac{1}{n}}$ for the calculation of adsorbed Fe-DMA complexes with Fe_{ads} as total adsorbed iron concentration [μmol g^{-1}], K_d as Freundlich distribution coefficient, *C* as dissolved iron equilibrium concentration [μmol] and n as correction factor

pH	K_d	1/n
5	1.15	1.11
6	1.14	0.86
7	0.17	1.19
8	1.15	1.11
9	0.40	0.54

The first 1 mL of the filtrate was discarded, 1 mL was collected for phytosiderophore analysis with HPLC and further 3 mL were collected for the measurement of dissolved iron with ICP-MS.

Analytical methods

Prior to the analysis of dissolved iron, the samples were stabilized by acidification with 30 μL of concentrated HNO_3 (Suprapur; Merck, Darmstadt, Germany). Total dissolved iron concentrations were measured with ICP-MS (Agilent 7500a). Standards were prepared by dilution of an iron atomic spectroscopy standard solution (Fluka, Buchs, Switzerland).

Phytosiderophore concentrations were measured with HPLC equipped with a Dionex AS11 anion exchange column (Dionex, Sunnyvale, USA) using an aqueous NaOH gradient, post-column derivatization, and fluorescence detection according to a method developed by Neumann et al. (1999). The post-column derivatization involves the oxidation of DMA by NaOCl (>12% Hypochlorite, Merck, Darmstadt, Germany) followed by labeling with the fluorophore OPA (orthophthaldialdehyde, Fluka, Buchs, Switzerland). In contrast to the method of Neumann et al. (1999), we did not use Brij-30 as constituent of the OPA solution. Prior to analysis, 20 μL of a 125 m*M* NaOH solution were added to 100 μL sample solution.

Results

Adsorption of DMA and Fe-DMA on goethite

The adsorption of phytosiderophores to iron oxide surfaces has been studied in order to gain a better understanding of their role in surface controlled dissolution mechanisms. The adsorption of DMA as a function of pH and of soluble DMA concentrations was measured. Adsorbed DMA concentrations decreased continuously with increasing pH (Figure 1). This is consistent with the adsorption behavior of many other organic ligands to hydrous iron oxides (Stumm, 1992).

Adsorption as a function of soluble DMA concentrations was recorded at pH 6 and 8 (Figure 2). We observed a non-linear increase of the DMA surface excess at both pH values. The DMA surface excess was higher at lower pH which is consistent with the data of the adsorption envelope (Figure 1). The observations were fitted with a Langmuir isotherm model (Sposito, 1989):

$$[\mathrm{DMA}]_{\mathrm{ads}} = \frac{b \cdot n_{\max} \cdot [\mathrm{DMA}]_{\mathrm{diss}}}{1 + b[\mathrm{DMA}]_{\mathrm{diss}}}, \qquad (1)$$

where $[\mathrm{DMA}]_{\mathrm{ads}}$ is the adsorbed DMA concentration, $[\mathrm{DMA}]_{\mathrm{diss}}$ is the dissolved DMA concentration, and $n_{\max}$ is the maximum surface excess of adsorbed phytosiderophores and b is an affinity parameter. The parameters b and $n_{\max}$ were fitted by least squares approximation of the

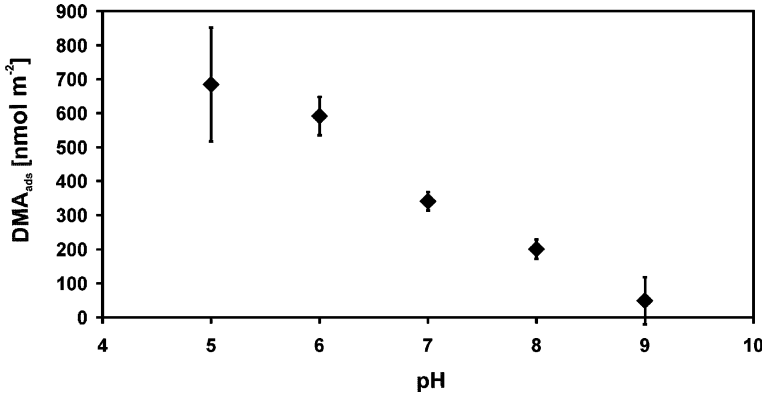

Figure 1. Adsorption envelope for DMA on goethite. Total DMA concentration: 500 m*M*, solids concentration: 2.5 g L^{-1}, background electrolyte: 0.01 *M* $NaNO_3$. Error bars show standard deviation (number of replicats: 2).

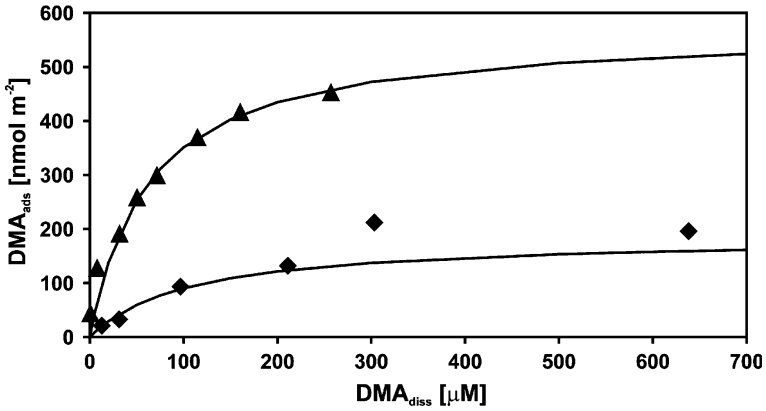

Figure 2. Adsorption isotherm for DMA on goethite at pH 6 (triangles) and pH 8 (diamonds). For pH 6: solids conc. 2.5 g L^{-1}, 0.01 *M* $NaClO_4$, 0.005 *M* MOPS. For pH 8: solids conc. 15 g L^{-1}, 0.01 *M* $NaNO_3$. Solid lines represent data fit with Langmuir isotherm model with calculated values for n_{max} = 570 nmol m^{-2} and b = 0.02 for pH 6 and n_{max} = 200 nmol m^{-2} and b = 0.01 for pH 8.

linearized form of the Langmuir equation. The maximum surface excess was calculated as 570 nmol m^{-2} at pH 6 (b = 0.02), and 200 nmol m^{-2} at pH 8 (b = 0.01).

The re-adsorption of soluble Fe-DMA complexes can have an important effect on the observation of iron oxide dissolution in batch experiments. Apparent dissolution rates are calculated based on observed changes of soluble iron over time. Corrected steady state dissolution rates can be calculated based on changes of soluble and re-adsorbed iron over time. Therefore, we investigated and quantified the adsorption of Fe-DMA complexes as a function of pH and of the concentration of the soluble complexes. For the pH-dependent adsorption of Fe-DMA complexes at the goethite surface (Figure 3), highest adsorbed concentrations were found at pH 5 and 6. In Figure 3a, the adsorption isotherms of Fe-DMA are plotted as adsorbed concentrations versus dissolved iron concentrations assuming that all dissolved iron added to the solution was complexed by DMA as predicted by speciation calculations. The adsorption of the Fe-DMA complexes increased with decreasing pH which is also reflected by the pH envelope of Fe-DMA adsorption onto goethite (Figure 3b). The observations of Fe-DMA adsorption onto goethite as a function of soluble Fe-DMA concentrations were fitted with a Freundlich isotherm model (Table 1).

Dissolution of goethite in the presence of phytosiderophores

Dissolution experiments at different adsorbed phytosiderophore concentrations and at different pH values were performed to elucidate the interplay between phytosiderophore adsorption and dissolution of iron oxides by phytosiderophores. Furthermore, the influence of the low molecular weight organic ligand oxalate on steady-state and non-steady-state goethite dissolution rates in the presence of phytosiderophores at pH 6 was investigated. DMA concentrations up to 3 m*M* were chosen for all dissolution experiments considering that Römheld (1991) estimated millimolar phytosiderophore concentrations in the rhizosphere around the root tip.

In the following discussion we distinguish between, 'apparent dissolution rates' (R^{app}) and, 'steady-state dissolution rates' (R^{SS}). Apparent dissolution rates are defined as the increase of soluble iron concentrations in batch dissolution experiments as a function of time. The apparent dissolution rates were determined from the slopes of the dissolution plots shown in Figure 4a using linear regression and subsequent normalization to the goethite surface area. Steady-state dissolution rates are defined as the increase of soluble iron plus re-adsorbed iron (as Fe-DMA complexes) as a function of time. The surface excess of re-adsorbed Fe-DMA complexes were

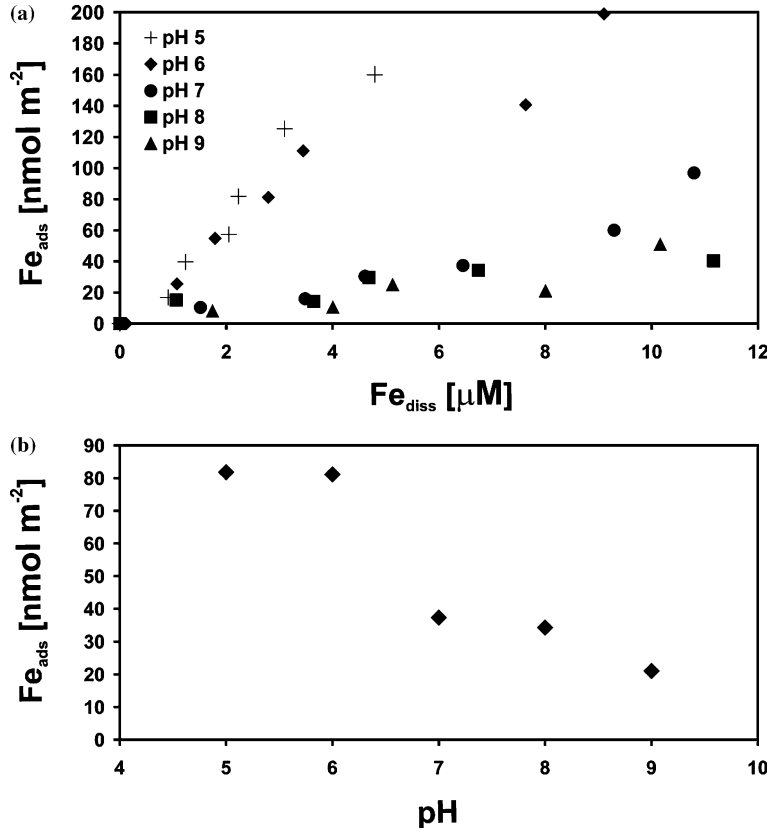

Figure 3. (a) Adsorption isotherms for Fe-DMA on goethite for pH 5, 6, 7, 8 and 9. Goethite solids conc. 2.5 g L^{-1}, 0.01 *M* $NaClO_4$, 0.005 *M* MOPS, 500 μM DMA, added Fe concentrations: 0, 3.5, 7, 10.5, 14, 21 and 28 μM for pH 6, and 0, 2.5, 5, 7.5, 10, 15 and 20 μM for pH 5, 7, 8 and 9. (b) pH-edge for Fe-DMA adsorption on goethite. Goethite solids conc.: 2.5 g L^{-1}, 0.01 *M* $NaClO_4$, 0.005 *M* MOPS, 10 μM Fe, 500 μM DMA.

calculated on the basis of the Freundlich isotherm models for Fe-DMA adsorption discussed above. Steady-state dissolution rates (R^{SS}, Figure 4b) were calculated by linear regression of the sum of dissolved and re-adsorbed Fe as a function of time.

Goethite dissolution rates were determined in the presence of five different DMA concentrations at pH 8 (Figure 4a). Apparent dissolution rates (R^{app}) and steady state dissolution rates (R^{SS}) increased with increasing total DMA concentrations.

Ligand promoted dissolution can be described by a rate law (Furrer and Stumm, 1986):

$$R_L^{SS} = k_L^{SS}[L]_{ads}, \qquad (2)$$

where R_L^{SS} is the overall steady-state ligand controlled dissolution rate [mol m^{-2} h^{-1}], k is a pseudo first-order dissolution rate coefficient [h^{-1}] and $[L]_{ads}$ is the ligand concentration [mol m^{-2}]. In this form, the rate law is valid only if the system is far from solubility equilibrium, and if other dissolution mechanisms (e.g., proton promoted or alkaline dissolution) have a negligible rate in this pH range. The linear relationship between steady-state dissolution rates of goethite in the presence of DMA and adsorbed DMA concentrations (Figure 4b) is consistent with the rate law (Equation 2), establishing a siderophore controlled dissolution mechanism. The slope of the curve shown in Figure 4b corresponds to the steady-state dissolution rate coefficient $k^{SS} = 0.0041\ h^{-1}$.

The influence of pH on goethite dissolution rates in the presence of 500 μM DMA was investigated for five different pH values (Figure 5). The highest apparent dissolution rate was observed at pH 7 (0.9 nmol m^{-2} h^{-1}) with

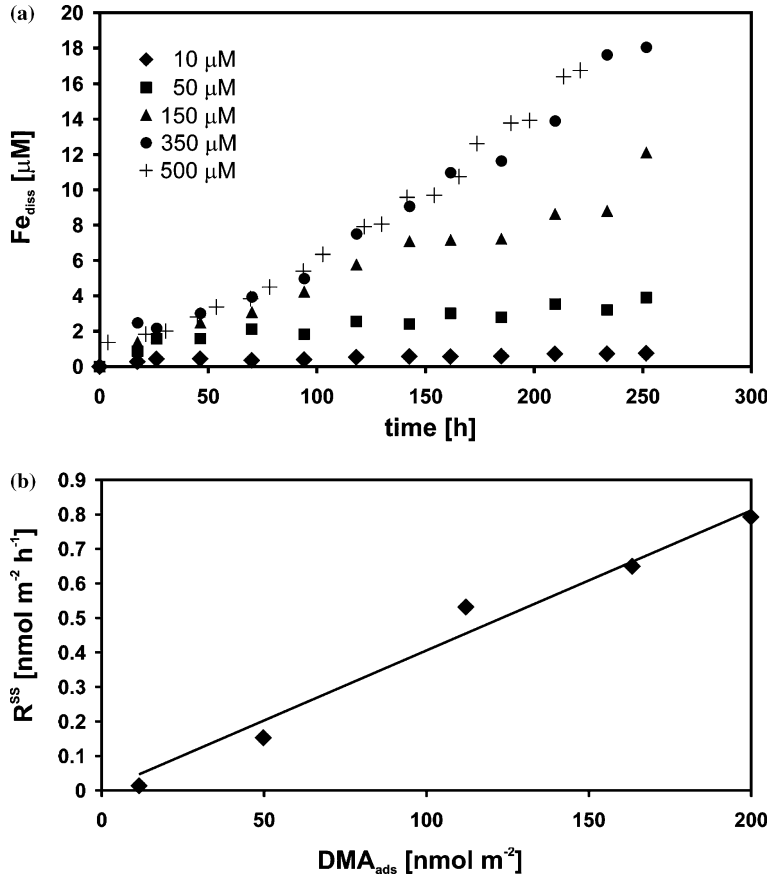

Figure 4. (a) Steady-state dissolution of goethite in the presence of different DMA concentrations at pH 8. DMA conc.: 10, 50, 150, 350 and 500 μM. Solids conc.: 2.5 g L^{-1}, 0.01 M $NaClO_4$, 0.005 M MOPS. (b) Steady-state dissolution rates R^{SS} *vs.* adsorbed DMA concentrations. Adsorbed DMA concentrations calculated with a Langmuir adsorption isotherm model (see Figure 2).

decreasing apparent rates toward more alkaline or acidic pH (R^{app}, Figure 6a). The lowest apparent dissolution rates were observed at pH 5 (0.12 nmol m^{-2} h^{-1}). In Figure 6a and b, the apparent dissolution rates R^{app}, the steady-state dissolution rates R^{SS} (calculated under consideration of Fe-DMA back-adsorption) and the steady-state dissolution rate coefficients (calculated by Equation 2) are plotted as a function of pH. From Figure 6a, it can be seen that the steady-state dissolution rates (R^{SS}, represented by diamonds) and the respective apparent dissolution rates (R^{app}, represented by squares) diverge from each other. For R^{SS}, highest values are calculated for pH 6 (R^{SS} = 1.7 nmol m^{-2} h^{-1}), with a sharp decline to pH 5 and a more moderate decline with increasing pH from 7 to 9.

In Figure 6b, the steady-state dissolution rate coefficients (for rate law Equation 2) are plotted as a function of pH. The rate coefficients increase with increasing pH. The rate coefficient for pH 9 was not calculated due to the high standard deviation of adsorbed DMA concentration at pH 9 (see Figure 1) resulting in an unacceptably high error in rate coefficients via error propagation.

The influence of organic ligands on DMA promoted dissolution of goethite

The influence of organic ligands on the dissolution kinetics of goethite in the presence of DMA was investigated for steady-state and non-steady-state conditions, using oxalate, a common soil constituent (Gadd, 2000), as model compound. Figure 7a, shows a comparison between steady-state dissolution of goethite at pH 6 in the presence of 0.5 mM DMA (diamonds), in the presence of 0.5 mM DMA and 0.1 mM oxalate

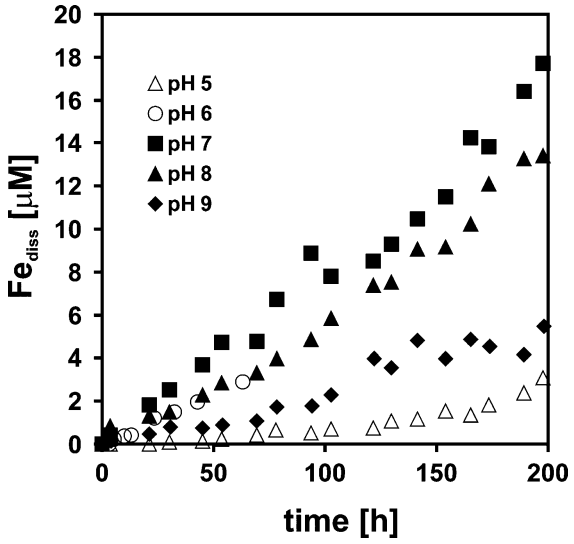

Figure 5. Steady-state dissolution of goethite in the presence of 500 μM DMA for different pH values. Solids conc.: 2.5 g L^{-1}, 0.01 M $NaClO_4$, 0.005 M MOPS.

(squares), and in the presence of 3 mM DMA and 0.1 mM oxalate (triangles). The slopes of the dissolution curves in Figure 7 represent the respective apparent dissolution rates for a goethite concentration of 2.5 g L^{-1}. The apparent dissolution rates for the three different steady-state dissolution experiments in Figure 7a were determined by linear regression. The presence of oxalate leads to an increase of the apparent dissolution rate for 0.5 mM DMA from R^{app}_{DMA} = 0.58 nmol m^{-2} $h^{-1}$to $R^{app}_{DMA,oxalate}$ = 0.97 nmol m^{-2} h^{-1} (Figure 7a). An increase of the DMA concentration to 3 mM at constant oxalate concentrations yield a further increase of the apparent dissolution rate to $R^{app}_{DMA,oxalate}$ = 1.6 nmol m^{-2} h^{-1}. Adsorption of oxalate at increasing DMA concentrations was investigated using ^{14}C-labeled oxalate. At a total oxalate concentration of 100 μM, an adsorbed oxalate concentration of 534.6 nmol m^{-2} was determined in the absence of DMA. Competitive adsorption of DMA lead to decreasing oxalate adsorption with

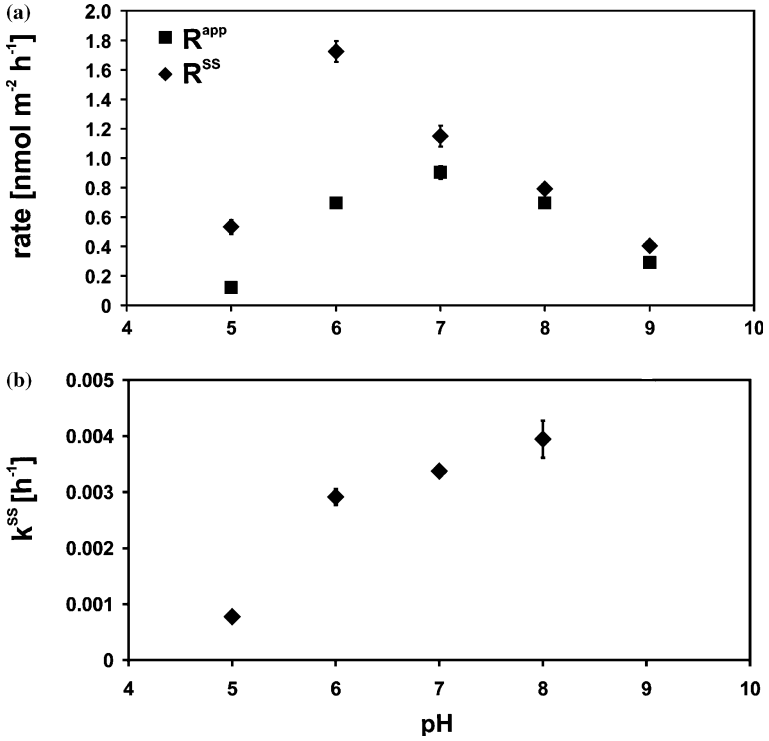

Figure 6. Steady-state dissolution rates R^{SS} corrected for adsorption of Fe-DMA and apparent dissolution rates R^{app} (a) and dissolution rate coefficient k^{SS} corrected for adsorption of Fe-DMA (b) for different pH values plotted against the respective pH. Error bars show standard deviation (number of replicats: 2).

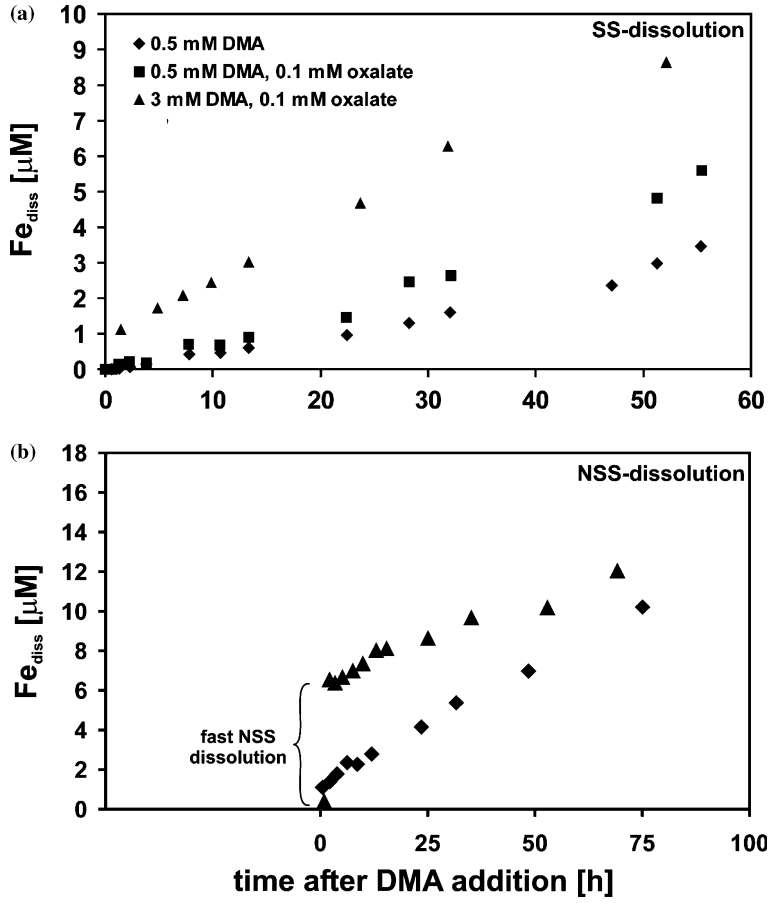

Figure 7. (a) Steady-state dissolution of goethite in the presence of 0.5 m*M* DMA (♦), in the presence of 0.5 m*M* DMA and 0.1 m*M* oxalate (■) and in the presence of 3 m*M* DMA and 0.1 m*M* oxalate (▲). (b) Non-steady-state dissolution of goethite in the presence of 3 m*M* DMA (♦) and in the presence of 3 m*M* DMA and 0.1 m*M* oxalate (▲). Time = 0 h is time of DMA addition. (♦): Goethite reacted without oxalate for 115 h. (▲): Goethite reacted with oxalate for 136 h. Solids conc.: 2.5 g L^{-1}, 0.01 *M* $NaClO_4$, 0.005 *M* MOPS, pH 6.

increasing DMA concentrations. At 0.5 m*M* DMA concentrations, oxalate adsorption decreased by 7%. At 3 m*M* DMA concentrations, oxalate adsorption decreased by 19%.

Non-steady-state dissolution of goethite in the presence of DMA and organic ligands

Non-steady-state dissolution experiments of goethite in the presence of DMA were carried out to investigate the effect of the diurnal pulse-like exudation of phytosiderophores observed for iron deficient graminaceous plants (Tagaki et al., 1984; Marschner et al., 1986) on the dissolution kinetics of iron oxides. Also, the effect of oxalate on non-steady-state dissolution was investigated. 0.1 m*M* oxalate were added at $t = 0$ h in one batch, whereas the other batch did not contain oxalate. Non-steady-state conditions were induced by the spike addition of 3 m*M* DMA after 115 h (no oxalate) or after 136 h (0.1 m*M* oxalate), in order to mimic a pulse-like root exudation behavior. The time of the addition of the DMA spikes corresponds to $t = 0$ h (Figure 7b). Notably, no dissolution of iron was observed before the addition of DMA in both non-steady-state experiments. In the absence of oxalate, the non-steady-state goethite dissolution rates after DMA addition are identical to apparent dissolution rates without oxalate (Figure 7a, diamonds) so that $R^{\mathrm{app}}_{\mathrm{DMA}} \approx R^{NSS}_{DMA} \approx 0.6$ nmol m^{-2} h^{-1} where R^{NSS}_{L} is

the apparent non-steady-state dissolution rate. Oxalate has a strong effect on the non-steady-state dissolution reaction. In the presence of oxalate, the pulse addition of DMA triggers a fast dissolution reaction that is subsequently followed by steady-state dissolution. The net rate of the fast non-steady-state dissolution reaction is much higher than steady-state rates: $R^{NSS}_{DMA,oxalate} = 24.7$ nmol m^{-2} h^{-1}. It is important to note that the non-steady-state dissolution rate can not be described by the rate law of steady-state dissolution from Equation 2. A reaction mechanism and rate law for non-steady-state ligand controlled dissolution has been elucidated by Reichard (2005). The fast non-steady-state dissolution reaction is followed by a slower dissolution reaction with similar net rates as the apparent steady-state dissolution in the presence of oxalate and DMA as measured before (Figure 7a, squares) with $R^{app}{}_{DMA,oxalate} = 0.8$ nmol m^{-2} h^{-1}.

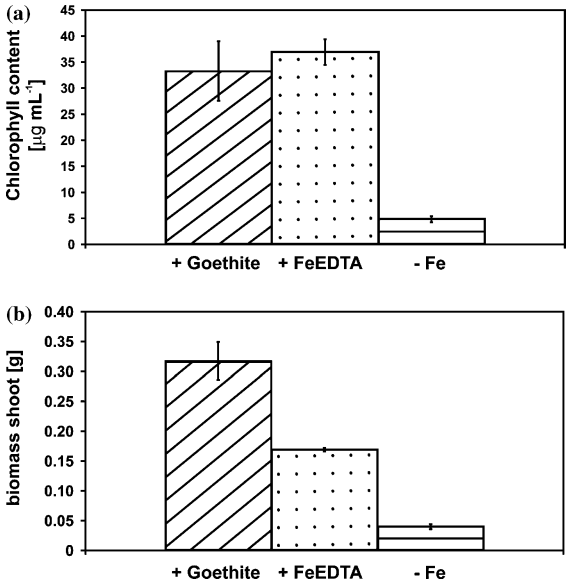

Figure 8. Comparison of the shoot biomass (g dry weight/plant) and chlorophyll content of wheat plants grown in hydroponic culture, 15 days after transplantation. The plants were exposed to goethite (+Goethite) or soluble Fe-EDTA (+Fe-EDTA) as sole iron source. A control experiment was conducted without iron in the nutrient solution (– Fe).

Plant growth experiments

In pot experiments, wheat plants were grown with three different iron treatments to investigate the bioavailability of goethite to wheat in comparison with Fe-EDTA, an iron source frequently used in growth experiments. The measured chlorophyll content of leaves and the biomass of the shoots of wheat plants of the three different treatments are shown in Figure 8. In contrast to the plants treated either with Fe-EDTA or goethite as iron-source, the plants without iron-source showed symptoms of iron deficiency (chlorosis). This was documented by the very low chlorophyll content measured in the leaves and was also reflected by low biomass production. The plants that were fed with goethite or Fe-EDTA showed no significant difference in the chlorophyll content. However, plants that were fed with Fe-EDTA showed a significantly lower biomass production of the shoot than the plants that had goethite as only iron-source.

Discussion

We found that adsorbed DMA concentrations decrease continuously with increasing pH as observed previously (Inoue et al., 1993). The adsorption envelope is typical for a ligand adsorbing to an oxide (Stumm et al. 1990) where an increase of negative surface charge in the neutral to alkaline pH range increases the standard free energy of adsorption of the negatively charged ligand. At constant pH of 6 and 8, Langmuir type adsorption isotherms were observed (Figure 2). The maximum DMA surface concentrations of 570 nmol m^{-2} at pH 6 and 200 nmol m^{-2} at pH 8 are well below the range of previously measured goethite surface site concentrations of 3 sites nm^{-2} ($\approx$ 5000 nmol m^{-2}) (Cornell and Schwertmann, 2003) but higher than the maximum surface concentrations of the microbial siderophores DFO-B (43 nmol m^{-2}) and DFO-D (100 nmol m^{-2}) on goethite at pH 6.6 (Kraemer et al., 1999).

Adsorption envelopes of the Fe-DMA complexes on goethite also show decreasing adsorption with increasing pH (Figure 3). Equilibrium calculations indicate that dissolved iron in solution is almost quantitatively complexed by DMA (Figure 9) and the solution is under-saturated with respect to iron oxides and hydroxides under the

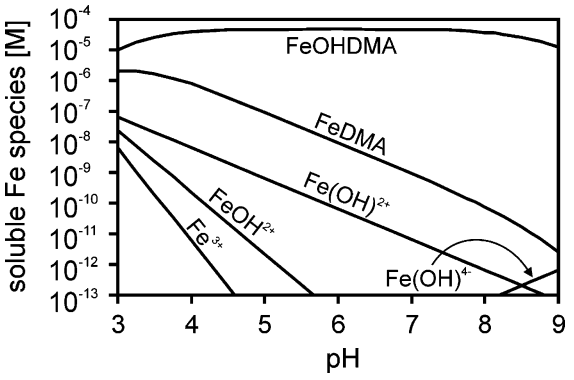

Figure 9. Stabilities of the dissolved Fe-DMA species for the pH range from 3 to 9 (for stability constants used for calculation see Table 2).

experimental conditions of adsorption experiments (PhreeqC, for thermodynamic equilibrium constants see Table 2). Inoue et al. (1993) also performed adsorption experiments with Fe-mugineic acid (MA) complexes and the iron oxides goethite, hematite, lepidocrocite and ferrihydrite. Compared to our data, Inoue et al. (1993) observed a much higher loss of Fe from solution. However, model calculations using published complex formation and solubility constants (Table 2) indicate that their system was strongly over-saturated with regard to all iron oxide phases with the exception of ferrihydrite. Thus, it is likely that their observation of high losses of iron from solution has been, at least to some extent, due to surface precipitation rather than adsorption.

The information on Fe-DMA adsorption on goethite allowed us to calculate concentrations of the products of the dissolution reaction, i.e. the sum of dissolved and adsorbed iron. Steady-state dissolution rates were then calculated as the increase of these products over time. The conceptual and quantitative separation of coupled processes including dissolution and adsorption is prerequisite for a mechanistic investigation of the dissolution process. It is important to note that the modeling of phytosiderophore promoted mobilization of iron in the rhizosphere will require the consideration of sorption processes not only to iron oxide surfaces, but to all potential adsorbates including oxides, clay minerals and humic substances.

A linear relationship between steady-state goethite dissolution rates and adsorbed DMA concentrations at pH 8 (Figure 4) is consistent with a ligand controlled dissolution mechanism and the corresponding rate law Equation 2 (Furrer and Stumm, 1986). However, plotting the dissolution rate coefficients as a function of pH shows that the dissolution coefficients are not constant in the pH range under investigation, but increase with increasing pH (Figure 6). Variations of dissolution rate coefficients with pH have previously been observed by Nowack and Sigg (1997) and by Whitehead (2003) for iron oxide dissolution in the presence of a range of other aminocarboxylate ligands. This was attributed to pH dependent changes in ligand surface speciation with increasing concentrations of a reactive surface species at elevated pH. The interplay between increasing rate coefficients and decreasing adsorbed DMA concentrations as a function of increasing pH results in maximum dissolution rates near neutral pH, which corresponds to the typical rhizosphere pH range in calcareous soils where iron deficiency typically occurs.

Table 2. Thermodynamic equilibrium constants at 298.15 K for the phytosiderophore deoxymugineic acid (DMA), Fe(III) and goethite

Reaction	Log K_{298}	Reaction	Log K_{298}
Deoxymugineic Acid		Fe(III)	
$H_4DMA^+ + H^+ = H_5DMA^{2+}$	2.13[b]	$Fe^{3+} + OH^- = FeOH^{2+}$	11.81[a]
$H_3DMA + H^+ = H_4DMA^+$	2.74[b]	$Fe^{3+} + 2\ OH^- = Fe(OH)_2^+$	23.40[a]
$H_2DMA^- + H^+ = H_3DMA$	3.41[c]	$Fe^{3+} + 4\ OH^- = Fe(OH)_4^-$	34.40[a]
$HDMA^{2-} + H^+ = H_2DMA^-$	8.69[c]	$2\ Fe^{3+} + 2\ OH^- = Fe_2(OH)_2^{4+}$	25.14[a]
$DMA^{3-} + H^+ = HDMA^{2-}$	10.66[c]	$3\ Fe^{3+} + 4\ OH^- = Fe_3(OH)_4^{5+}$	49.70[a]
$DMA^{3-} + Fe^{3+} = FeDMA$	20.36[c]	*Goethite*	
$DMA^{3-} + Fe^{3+} + H_2O = FeOHDMA^- + H^+$	18.01[c]	$2\ H_2O + Fe^{3+} = FeOOH(s) + 3H^+$	−0.36[d]

Conditional equilibrium constants from [a] Martell et al. (2001); [b] von Wirén et al. (2000); [c] Murakami et al. (1989); [d] Parker and Khodakovskii (1995). Corrected to zero ionic strength with Davies equation.

At concentrations typically found in the rhizosphere, non-siderophore ligands such as oxalate have a negligible effect on the solubility of crystalline iron oxides in the neutral pH range due to their low affinity for iron versus the high thermodynamic stability of the oxides (Eick et al., 1999; Cheah et al., 2003; Reichard, 2005). However, we observed that oxalate increases the apparent steady-state dissolution rate of goethite in the presence of low phytosiderophore concentrations (Figure 7a). Such synergistic effects between siderophores and non-siderophore ligands have also been observed by Cheah et al. (2003) (oxalate and the microbial siderophore desferrioxamine B (DFO-B)) and Reichard (2005) (oxalate, malonate, fumarate, or succinate and DFO-B). They attributed the synergistic effect to an increase of the iron solubility by the siderophore which provides the thermodynamic driving force to dissolution mechanisms involving the non-siderophore ligand (Kraemer, 2004). This suggests that the co-exudation of low molecular weight organic ligands by iron deficient grasses (Fan et al., 1997) could enhance phytosiderophore promoted iron mobilization in the rhizosphere. Fan et al. (1997) found that in the early stage or at low levels of iron deficiency, barley plants exuded higher concentrations of low molecular weight organic ligands than of phytosiderophores. At a high level of iron stress, the exudation of organic ligands was reduced and the production of phytosiderophores became dominant.

It is intriguing to consider that synergistic effects, which we observed in dissolution experiments involving relatively low DMA and oxalate concentrations, is exploited by plant exuding mixtures of phytosiderophores and low molecular weight organic ligands. Based on our experiments (Figure 6a) we can speculate that further increases of dissolution rates are promoted by exuding almost exclusively phytosiderophores at high exudation rates under strongly iron deficient conditions (Fan et al., 1997) with a disadvantage of the metabolic cost of synthesizing phytosiderophores at high rates.

Hitherto, considerations for the dissolution of goethite by phytosiderophores were made for steady-state conditions. However, in the rhizosphere of plants, non-steady-state conditions are commonly induced by plant and microbial growth and decay processes and diurnal variations of nutrient and water uptake or exudation of biogenic substances. Takagi et al. (1984) and Römheld and Marschner (1986), for example, described a diurnal rhythm of the phytosiderophore exudation by graminaceous plants. This exudation pattern seems to have several advantages for the plant. Rapid release rates lead to high phytosiderophore concentrations in the rhizosphere during the period of maximum exudation (Römheld, 1991). It has been suggested that the resulting strong variations of siderophore concentrations in the rhizosphere reduce their microbial degradation (Darrah, 1991; Römheld, 1991). Mori (1994) noted that high transient concentrations may also allow the phytosiderophore to compete for iron complexation with microbial siderophores that usually have higher affinity for iron (e.g., DFO-B: $\log K_{FeHDFO^+} = 30.6$ (Schwarzenbach and Schwarzenbach, 1963)). The timing of maximum phytosiderophore exudation around noon corresponds to maximum plant transpiration rates which create advectional flow of soil water towards the root. Hence, the radial diffusive transport of siderophores away from the root is countered by advective transport toward the root, providing an efficient retrieval mechanism for iron siderophore complexes (Takagi, 1991).

To investigate the effect of the diurnal phytosiderophore release on goethite dissolution rates, we performed non-steady-state dissolution experiments in the presence and absence of 0.1 mM oxalate (Figure 7b). Non-steady-state was induced by spike additions of 3 mM DMA. In the absence of oxalate, no fast non-steady-state dissolution of goethite is observed. However, in the presence of oxalate, the addition of DMA triggered a fast non-steady-state dissolution reaction (Figure 7b). Such fast non-steady-state dissolution reactions as a response to pulse additions of siderophores have been observed previously (Reichard, 2005). Reichard (2005) elucidated the mechanism of this non-steady-state reaction and developed a four-step-model:

$$\equiv Fe - OH + HL \overset{fast}{\leftrightarrow} \equiv Fe - L + H_2O \qquad (3)$$

$$\equiv Fe - L \underset{k_{-1}}{\overset{k_1}{\leftrightarrow}} \equiv Fe - L_{lab} \qquad (4)$$

$$Fe - L_{lab} \underset{k_{-2}}{\overset{k_2}{\leftrightarrow}} Fe - L_{diss} \quad (5)$$

$$Fe - L_{diss} + HSid \overset{fast}{\leftrightarrow} Fe - Sid_{diss} + HL \quad (6)$$

The first step involves the fast adsorption of a ligand (e.g., oxalate) at the goethite surface by a ligand-exchange reaction of surface hydroxyl-groups (Equation 3). The second step (Equation 4) consists of the slow, ligand controlled generation of a kinetically labile iron pool at the mineral surface before the addition of the siderophore. In the following, the concentration of this labile pool increases with increasing reaction time of the adsorbed organic ligand at the iron oxide surface. An accumulation of labile iron surface sites occurs due to the low equilibrium concentration of dissolved iron in the presence of the organic ligand (Equation 5). As a last step (Equation 6), the addition of a non-steady-state phytosiderophore concentration leads to an increase of the iron solubility and the labile iron pool is therefore rapidly released. On the basis of these four reaction steps, Reichard (2005) modeled the non-steady-state dissolution behavior in the presence of the siderophore desferrioxamine B and oxalate.

These observations suggest that diurnal variations in phytosiderophores root exudation rates trigger fast non-steady-state dissolution reactions which allow efficient plant iron acquisition from crystalline iron oxides. Furthermore, non-siderophore organic ligands which are co-exuded by iron stressed plants or by rhizosphere bacteria or fungi, can have synergistic effects on the dissolution of iron oxides (Reichard, 2005).

The non-steady-state dissolution experiments presented here have been conducted at pH 6. In calcareous soils, the pore water pH is controlled by the solubility of calcite and the CO_2 partial pressure in the gas phase. In the presence of pure calcite and at atmospheric CO_2 partial pressure ($10^{-3.5}$ atm) the calculated equilibrium pH is 8.3. However, observed CO_2 partial pressures in the rhizosphere are significantly higher ($10^{-1.2} - 10^{-0.9}$ atm) due to respiration by plant roots and microorganisms (Gollany et al., 1993). The calculated equilibrium pH at such elevated CO_2 partial pressures is between pH 6.5 and 7. Future work on non-steady state dissolution processes should address the effect of pH in this range on dissolution rates.

In previous studies, crystalline iron oxides such as goethite were usually not considered to contribute to plant available iron, although, for example, Bertrand and Hinsinger (2000) found a re-greening of iron deficient maize by growing the plants on a substrate consisting of a mixture of synthesized goethite and quartz sand. Due to the lower iron dissolving ability of maize compared to the dicots rape or pea, they concluded that maize did only dissolve minor concentrations of crystalline goethite, but mainly dissolved amorphous impurities in the goethite. In the pot experiment represented here, we investigated iron acquisition from goethite by wheat plants. Wheat is known to secrete larger amounts of phytosiderophores than maize (Römheld, 1991; Marschner, 1995). We demonstrated that wheat plants were able to acquire iron by dissolving goethite when used as the sole iron source. Also, shoot biomass was greater when using goethite as iron source complared to Fe-EDTA treatments as shown in Figure 8b. This is consistent with observations by Rengel (2002) who reported on the decreased growth of wheat grown in nutrient solutions with EDTA chelator compared with foliar spray supply of Fe. Trace contaminations of the goethite with amorphous Fe-hydroxides contaminations can not be detected by XRD and BET measurements that we used to characterize the synthesized goethite. However, such contaminations would have been evidenced in the dissolution experiments by fast initial dissolution reactions (dominated by fast dissolution of the labile pool) followed by a decrease of dissolution rates (dominated by slow dissolution of goethite). This has not been observed in our dissolution study (see Figure 7a) since we see very little fast-initial dissolution and the dissolution rates remained essentially constant over the course of the experiment. From the steady-state dissolution of goethite in the presence of DMA (Figure 7a), it was found that the concentration of iron released in a fast initial dissolution process depends on the concentration of added DMA. In the steady-state dissolution experiment shown in Figure 7a, no fast initial dissolution of iron was observed at a DMA concentration of 0.5 m*M*. Römheld (1991) estimated phytosiderophore

concentrations in the rhizosphere around the roots of maximum 1 m*M*. Thus, it is assumed that iron from a fast initial dissolution is negligible as iron source for the plant. However, fast-initial dissolution of crystalline minerals is commonly observed (Cornell and Schwertmann, 2003) and non-steady-state dissolution processes are triggered by changes in pH (Samson and Eggleston, 2000) and ligand concentrations (as shown above). These processes can be seen as typical reactions on crystalline iron oxides surfaces that increase their bioavailability and are likely to contribute to plant iron acquisition. Therefore, we propose that wheat is able to dissolve iron from crystalline iron oxide phases such as goethite. The mechanism of iron oxide dissolution in the rhizosphere cannot be inferred from iron uptake experiments. However, it is likely that phytosiderophore promoted steady-state and non-steady-state dissolution mechanisms that we elucidated in this study may contribute to the high iron efficiency of graminaceous plants.

Acknowledgements

We are indebted to Prof. Volker Römheld and Dr. Günther Neumann (Universität Hohenheim) for introducing us to phytosiderophore purification and analysis methods and for many enlightening discussions of plant iron acquisition. Also, we want to thank Kurt Barmettler for sharing his experience in analytical chemistry, and Regula Bollier, Dominique Gärtner, and Felix Weber for their assistance in the lab. The manuscript greatly benefited from the detailed and constructive criticism of two anonymous reviewers. This work was supported by the Swiss Federal Institute of Technology, ETH project # 7159.

References

Alam S, Akiha F, Kamei S and Kawai S 2004 Diurnal variations in absorption and translocation of a ferrated phytosiderophore in barley as affected by iron deficiency. J. Soil Sci. Plant Nutr. 50, 457–461.

Awad F, Römheld V and Marschner H 1994 Effect of root exudates on mobilization in the rhizosphere and uptake of iron by wheat plants. Plant and Soil 165, 213–218.

Bertrand I and Hinsinger P 2000 Dissolution of iron oxyhydroxide in the rhizosphere of various crop species. J. Plant Nutr. 23, 1559–1577.

Cheah S F, Kraemer S M, Cervini-Silva J and Sposito G 2003 Steady-state dissolution kinetics of goethite in the presence of desferrioxamine B and oxalate ligands: implications for the microbial acquisition of iron. Chem. Geol. 198, 63–75.

Cornell R M and Schwertmann U 2003 The Iron Oxides. Wiley-VCH, Weinheim.

Dakora F D and Phillips D A 2002 Root exudates as mediators of mineral acquisition in low-nutrient environments. Plant and Soil 245, 35–47.

Darrah P R 1991 Models of the rhizosphere. 1. Microbial-population dynamics around a root releasing soluble and insoluble carbon. Plant and Soil 133, 187–199.

Eick M J, Peak J D and Brady W D 1999 The effect of oxyanions on the oxalate-promoted dissolution of goethite. Soil Sci. Soc. Am. J. 63, 1133–1141.

Fan T W M, Lane A N, Pedler J, Crowley D and Higashi R M 1997 Comprehensive analysis of organic ligands in whole root exudates using nuclear magnetic resonance and gas chromatography mass spectrometry. Anal. Biochem. 251, 57–68.

Filius J D, Hiemstra T and van Riemsdijk W H 1997 Adsorption of small weak organic acids on goethite: Modeling of mechanisms. J. Colloid Interf. Sci. 195, 368–380.

Furrer G and Stumm W 1986 The coordination chemistry of weathering: 1 Dissolution kinetics of δ-Al_2O_3 and BeO. Geochim. Cosmochim. Acta 50, 1847–1860.

Gadd G M 2000 Heterotrophic solubilization of metal-bearing minerals by fungi. *In* Environmental Mineralogy. Eds. J D Cotter-Howells, D L S Campbell, E Valsami-Jones and M Batchelder. pp 57–75. The Mineralogical Society, London.

Gollany H T, Schumacher T E, Rue R R and Liu S-Y 1993 A carbon dioxide microelectrode for in situ pCO_2 measurement. Microchem. J. 48, 42–49.

Graustein W C and Cromack K 1977 Calcium oxalate: Occurrence in soils and effect on nutrient and geochemical cycles. Science 198, 1252–1254.

Hagström J, James W M and Skene K R 2001 A comparison of structure, development and function in cluster roots of Lupinus albus L. under phosphate and iron stress. Plant and Soil 232, 81–90.

Higuchi K, Suzuki K, Nakanishi H, Yamaguchi H, Nishizawa N K and Mori S 1999 Cloning of nicotianamine synthase genes, novel genes involved in the biosynthesis of phytosiderophores. Plant Physiol. 119, 471–479.

Higuchi K, Watanabe S, Takahashi M, Kawasaki S, Nakanishi H, Nishizawa N K and Mori S 2001 Nicotianamine synthase gene expression doffers in barley and rice under Fe-deficient conditions. Plant J. 25, 159–167.

Hiradate S and Inoue K 1998 Dissolution of iron from iron (hydr)oxides by mugineic acid. Soil Sci. Plant Nutr. 44, 305–313.

Inoue K, Hiradate S and Takagi S 1993 Interaction of mugineic acid with synthetically produced iron-oxides. Soil Sci. Soc. Am. J. 57, 1254–1260.

Jones D L 1998 Organic acids in the rhizosphere – a critical review. Plant and Soil 205, 25–44.

Jones D L and Brassington D S 1998 Sorption of organic acids in acid soils and its implications in the rhizosphere. Europ. J. Soil Sci. 49, 447–455.

Jones D L, Darra P R and Kochian L V 1996 Critical evaluation of organic acid mediated iron dissolution in the

rhizosphere and its potential role in root iron upake. Plant and Soil 180, 57–66.
Kraemer S M 2004 Iron oxide dissolution and solubility in the presence of siderophores. Aquat. Sci. 66, 3–18.
Kraemer S M, Cheah S F, Zapf R, Raymond K N and Sposito G 1999 Effect of hydroxamate siderophores on Fe release and Pb(II) adsorption by goethite. Geochim. Cosmochim. Acta 63, 3003–3008.
Large E C 1954 Growth stages in cereals. Plant Pathol. 3, 128–129.
Lindsay W L 1979 Chemical Equilibria in Soils. Wiley Interscience, New York.
Ma J F and Nomoto K 1996 Effective regulation of iron acquisition in graminaceous plants The role of mugineic acids as phytosiderophores. Physiol. Plant. 97, 609–617.
Ma J F, Shinada T, Matsuda C and Nomoto K 1995 Biosynthesis of phytosiderophores, mugineic acids, associated with methionine cycling. J. Biol. Chem. 270, 16549–16554.
Ma JF, Ueno H, Ueno D, Rombolà A D and Iwashita T 2003 Characterization of phytosiderophore secretion under Fe deficiency stress in *Festuca rubra*. Plant and Soil 256, 131–137.
Marschner H 1995 Mineral Nutrition of Higher Plants. 2ndAcademic Press, London.
Marschner H, Römheld V and Kissel M 1986 Different strategies in higher-plants in mobilization and uptake of iron. J. Plant Nutr. 9, 695–713.
Marschner H, Römheld V and Kissel M 1987 Localization of phytosiderophore release and of iron uptake along intact barley roots. Phys. Plant. 71, 157–162.
Martel A E, Smith R M and Motekaitis R J 2001 NIST Critically selected Stability Constants of Metal Complexes. NIST Standard reference database 46. Version 6.0, Gaithersburg, NIST.
Matar A, Torrent J and Ryan J 1992 Soil and fertilizer phosphorous and crop responses in the dryland mediterranean zone. Adv. Soil Sci. 18, 81–146.
Moran R 1982 Formulae for determination of chlorophyllous pigments extracted with N,N-dimethylformamide. Plant Physiol. 69, 1376–1381.
Mori S 1994 Mechanism of iron acquisition by graminaceous (strategy II) plants. *In* Biochemistry of Metal Micronutrients in the Rhizosphere. Ed. J A Manthey, D E Crowley and D G Luster pp. 225–249. Lewis, Boca Raton.
Murakami T, Ise K, Hayakawa M, Kamei S, Takagi S, 1989 Stabilities of Metal Complexes of Mugineic acids and their specific affinities for iron (III). Chem Lett. 2137–2140.
Nakanishi H, Bughio N, Matsuhashi S, Ishioka N, Uchida H, Tsuji A, Osa A, Sekine T, Kume T and Mori S 1999 Visualizing real time [^{11}C]methionine translocation in Fe-sufficient and Fe-deficient barley using a positron emitting tracer imaging system (PETIS). J. Exp. Bot. 50, 637–643.
Negishi T, Nakanishi H, Yazaki J, Kishimoto N, Fujii F, Shimbo K, Yamamoto K, Sakata K, Sasaki T, Kikuchi S, Mori S and Nishizawa N K 2002 cDNA microarray analysis of gene expression during Fe-deficiency stress in barley suggests that polar transport of vesicles is implicated in phytosiderophore secretion in Fe-deficient barley roots. Plant J. 30, 83–94.
Neumann G, Haake C and Römheld V 1999 Improved HPLC method for determination of phytosiderophores in root washings and tissue extracts. J. Plant Nutr. 22, 1389–1402.
Nowack B and Sigg L 1997 Dissolution of Fe(III)(hydr)oxides by metal-EDTA complexes. Geochim. Cosmochim. Acta 61, 951–963.
Parker VB and Khodakovskii IL 1995 Thermodynamic properties of The aqueous ions (2+ and 3+) of iron and The key Compounds of iron. J. Phys. Chem. Ref. Data 24, 1699–1745.
Parkhurst D L and Appelo C A J 1999 Users Guide to PhreeqC (Version 2) – A computer program for speciation, batch-reaction, one-dimensional transport, and inverse geochemical calculations. U.S. Geological Survey Water-Resources Investigations Report, Denver, Colorado 99–4259.
Reichard P U 2005 Effects of microbial and plant siderophore ligands on the dissolution of iron oxides. Ph.D. Thesis # 15665 Swiss Federal Institute of Technology, Zurich, Switzerland.
Rengel Z 2002 Chelator EDTA in nutrient solution decreases growth of wheat. J. Plant Nutr. 25, 1709–1725.
Römheld V 1991 The role of phytosiderophores in acquisition of iron and other micronutrients in graminaceous species: An ecological approach. Plant and Soil 130, 127–134.
Römheld V and Marschner H 1986 Evidence for a specific uptake system for iron phytosiderophores in roots of grasses. Plant Physiol. 80, 175–180.
Samson S D and Eggleston CM 2000 The depletion and regeneration of dissolution-active sites at the mineral-water interface: II. Regeneration of active sites on α-Fe2O3 at pH 3 and pH 6. Geochim. Cosmochim. Acta 64, 3675–3683.
Schwarzenbach G and Schwarzenbach K 1963 Hydroxamatkomplexe. 1. Die Stabilität der Eisen(III)-Komplexe einfacher Hydroxamsäuren und des Ferrioxamins B. Helvet. Chim. Acta 46, 1390–1400.
Schwertmann U and Cornell R M 2000 Iron Oxides in the Laboratory: Preparation and Characterization. Wiley-VCH, Weinheim.
Singh K, Sasakuma T, Bughio N, Takahashi M, Nakanishi H, Yoshimura E, Nishizawa N K and Mori S 2000 Ability of ancestral wheat species to secrete mugineic acid family phytosiderophores in response to iron deficiency. J. Plant Nutr. 23, 1973–1981.
Sposito G 1989 The chemistry of soils. Oxford University Press, Oxford.
Stewart J D and Lieffers V J 1994 Diurnal cycles of rhizosphere acidification by *Pinus contorta* seedlings. Plant and Soil 162, 299–302.
Strobel B W 2001 Influence of vegetation on low-molecular-weight carboxylic acids in soil solution – a review. Geoderma 99, 169–198.
Stumm W 1992 Chemistry of the Solid-Water Interface. Wiley-Interscience, New York.
Stumm W, Sulzberger B and Sinninger J 1990 The coordination chemistry of oxide-electrolyte interface; the dependence of surface reactivity (dissolution, redox reactions) on surface structures. Croat. Chem. Acta 63, 277–312.
Sugiura Y and Nomoto K 1984 Phytosiderophores - structures and properties of mugineic acids and their metal complexes. Struct. Bond. 58, 107–135.
Takagi S 1991 Mugineic acids as example of root exudates which play an important role in nutrient uptake by plant roots. *In* Phosphorus Nutrition of Grain Legumes in the Semi-Arid Tropics. Eds. C Johansen, KK Lee and K L Sahrawat pp. 77–90. ICRISAT, Patancheru.

Takagi S 1993 Production of phytosiderophores. *In* Iron Chelation in Plants and Soil Microorganisms. Eds. LL Barton and BC Hemming pp. 111–131. Academic Press, San Diego.

Takagi S, Nomoto K and Takemoto T 1984 Physiological aspect of mugineic acid, a possible phytosiderophore of graminaceous plants. J. Plant Nutr. 7, 469–477.

Takagi S, Kamei S and Yu M 1988 Efficiency of iron extraction from soil by mugineic acid family phytosiderophores. J. Plant Nutr. 11, 643–651.

Vančura V 1964 Root exudates of plants. Plant and Soil 21, 231–248.

Von Wirén N, Khodr H and Hider RC 2000 Hydroxylated Phytosiderophore Species Possess an enhanced Chelate Stability and affinity for iron (III). Plant Physiol 124, 1149–1157.

Whitehead C F 2003 (Amino)carboxylate coordination reactions with ferric (hydr)oxides: Adsorption and ligand-assisted dissolution. Ph.D. Thesis. Johns Hopkins University, Baltimore, USA.

Yehuda Z, Shenker M, Römheld V, Marschner H, Hadar Y and Chen Y N 1996 The role of ligand exchange in the uptake of iron from microbial siderophores by gramineous plants. Plant Phys. 112, 1273–1280.

Yu Q Y, Kandegedara A, Xu Y and Rorabacher D B 1997 Avoiding interferences from Good's buffers: A contiguous series of non-complexing tertiary amine buffers covering the entire range of pH 3–11. Anal. Biochem. 253, 50–56.

Section editor: H. Lambers